S1 Methods

S1.1 Information on sampling stations

Table S1 Name, waterscape and geographical location of all investigated sampling stations. R indicates river stations, C are channel stations and L represent lake stations. Station 16 was sampled only once due to insufficient accessibility by motor boat and is therefore excluded from the dataset in this paper.

Station	waterscape	Name	latitude	longitude
1	R	Patlageanca	45.21841	28.75167
2	R	Mila 35	45.19757	28.87490
3	R	Chilia [a]	45.25218	29.66011
4	R	Sulina [b]	45.16231 * 45.15790**	29.72729 * 29.63783**
5	R	St. Gheorge	44.89552	29.58627
6	C	Channel St. Gheorge	44.90902	29.58842
7	L	Lake Puiu	45.05563	29.48437
8	L	Lake Rosu	45.05398	29.56852
9	C	Channel Sulina	45.15544	29.61046
10	C	Channel Impututa	45.12802	29.59182
11	C	Old Danube M2	45.18104	29.47730
12	R	Crisan	45.17247	29.47278
13	L	Lake Bogdaproste	45.23381	29.35933
14	L	Lake Isac	45.11264	29.27449
15	R	Murighiol	45.04322	29.19678
16	*L*	*Lake Tataru*	*45.03686*	*29.61423*
17	C	Old Danube M1	45.18274	29.34535
18	C	Caraorman Channel	45.12280	29.38938
19	L	Lake Uzlina	45.09096	29.26453
20	L	Lake Rosulet	45.07309	29.61386

[a] Due to the border with Ukraine, this station had to be shifted to a small side branch of the Chilia branch. Comparative measurements showed no difference from the main branch.
[b] The Sulina station was shifted upstream end of February 2016, since a continuously measuring sensor indicated influence of the Black Sea water: * old location, ** new location

S1.2 Evaluation of CH_4 fluxes

The following examples document the evaluation of CH_4 fluxes from discrete samples (Fig S1), which were measured using GC-FID (Aglient Technologies, USA). Continuous measurements (Fig. S2) in the headspace of the chamber were performed with an Ultraportable CH_4/N_2O analyzer (Los Gatos Research, USA).

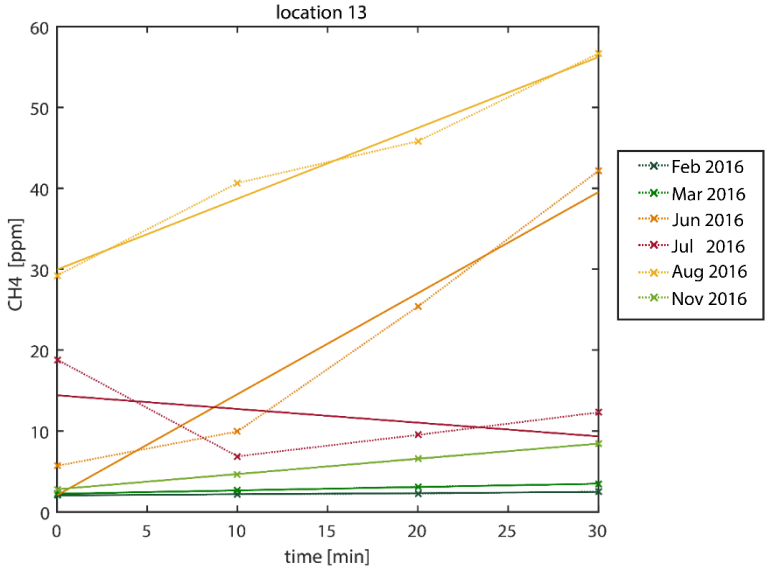

Figure S1 Flux measurements at location 13 highlighting the 3 different cases encountered during data evaluation. Dotted lines link individual measurements (x), solid lines show the calculated regression line. Green: linear fluxes with $R^2 > 0.96$, which we interpreted as diffusive CH_4 fluxes. Yellow and orange: fluxes that had an $R^2 < 0.96$ and therefore were categorized to show signs of ebullition. Estimated fluxes were therefore reported as total fluxes. The diffusive contribution was estimated from CH_4 water concentration and k_{600}, which we derived from CO_2 flux measured at the respective time and location. Dark red: non-monotonous flux, either by capturing a bubble or mislabelling a sample. Such time-series were not included in the further analysis.

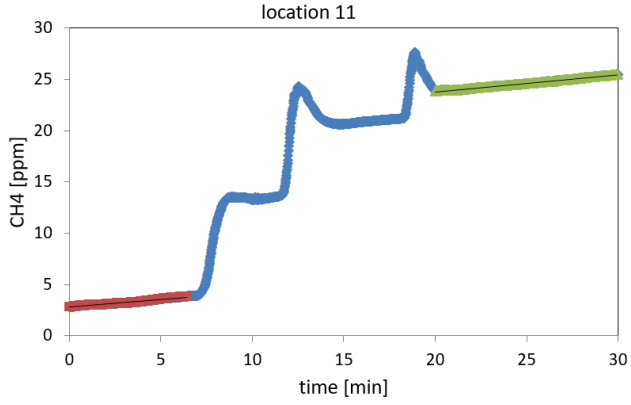

Figure S2 Continuous flux measurement with the Ultraportable CH_4/N_2O analyser at location 11 in September 2017. Diffusive fluxes are indicated in red and green, while the blue section shows sharp increases that indicate ebullition. Depending on the ebullitive flux, the system responded with overshooting. Diffusive fluxes were determined via the slope of the regression line of intervals where no influence of ebullition was observed. The total flux was determined by the overall concentration increase during the observed time interval.

S2 Results

S2.1 Comparison of observed temperature and conductivity to long-term data from ICPDR

Comparison of our measurements upstream of Tulcea with long-term observations from Reni (data from ICPDR, 2018) show that our observations are well within the range of previous measurements (Figure S3). Temperature was warmer in July, August and September 2016 and 2017 than the long-term average.

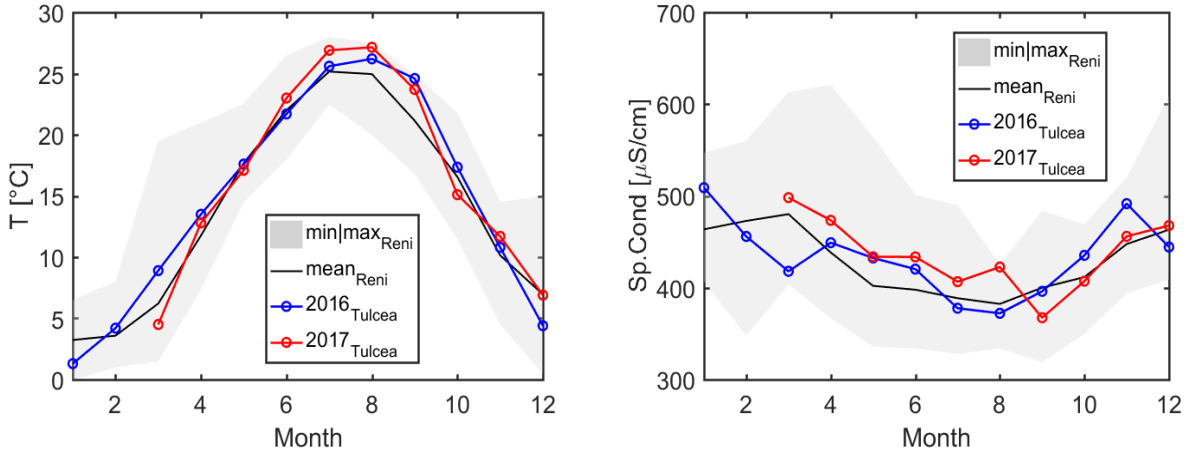

Figure S3 Seasonal development of temperature and specific conductivity. The blue and red line show our monthly observations in the Danube upstream of Tulcea in 2016 and 2017, respectively. The black line represents the average of monthly to biweekly measurements in the period January 1996 to December 2014 in the case of temperature and July 1996 to December 2014 in the case of specific conductivity (ICPDR, 2018).

S2.2 Visual results of Kruskal-Wallis Test

We visualized the results of the multiple comparison test after Dunn-Sidak based on statistical data obtained from the Kruskal-Wallis test using the multcompare function in Matlab. Most parameters are significantly different in the channels and lakes within the Danube delta compared to the river reaches outside. The time series of POC seems to be similar in lakes and the river, however closer inspection indicates that this coincidence may be caused by different POC sources, specifically the spring peak during high sediment transport in the river and the summer peak during algal bloom in the delta lakes.

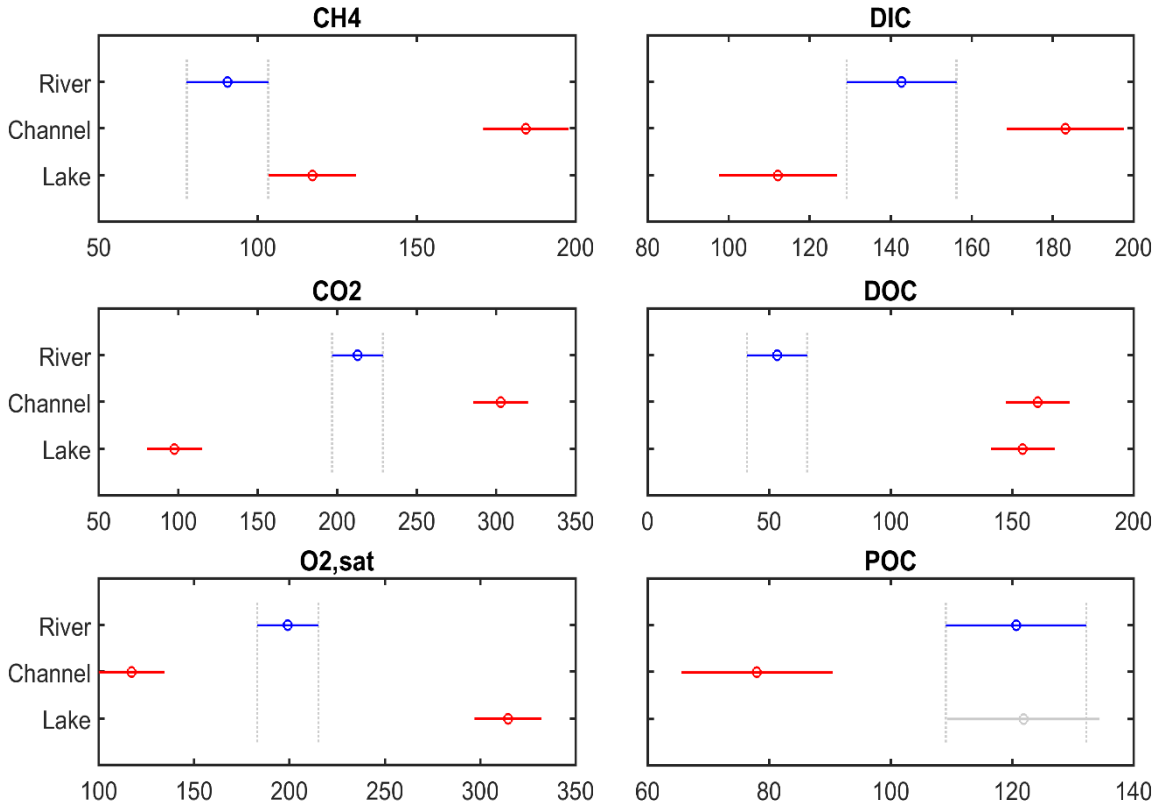

Figure S4 Visualization of results from Kruskal-Wallis non-parametric test for equal medians followed by Dunn-Sidak multiple comparison testing. Circles indicate the group mean, non-overlapping horizontal bars show significant difference: The channels and lakes in red are significantly different from the blue river group. Grey indicates no significant difference. The x-axis shows the average group ranks from the Kruskal-Wallis test.

S3 Discussion

S3.1 CO_2 and CH_4 fluxes upscaled for three different waterscapes

In the main text, Figure 5 illustrates the CO_2 and CH_4 fluxes from the different waterscapes to the atmosphere estimated from our monthly measurements. Below, Table S2 displays the numbers that are underlying the bar graphs in Figure 5, where the height of the bar indicates results based the median fluxes, while the minimum and maximum extension of the black lines show the range resulting from calculations with 25 and 75 percentiles, respectively.

Table S2 Total CO_2 and CH_4 emissions (GgC yr^{-1}) from the three waterscapes of the Danube Delta in 2016 and 2017. For CH_4 both diffusive and total fluxes are displayed. Because of large gaps in CH_4 data no fluxes were calculated for 2017.

Flux	River		Channel		Lake		Total	
[GgC yr^{-1}]	median	range	median	range	median	range	median	range
$CO_{2,\ 2016}$	22	16–30	19	12–36	19	4.6–45	59	32–111
$CO_{2,\ 2017}$	18	15–22	8.4	3.0–19	-3.3	-15–12	23	3.2–54
$CH_{4,\ dif,\ 2016}$	0.25	0.13–0.36	0.16	0.11–0.48	0.79	0.52–1.9	1.2	0.76–2.8
$CH_{4,\ tot,\ 2016}$	0.25	0.15–0.39	0.22	0.13–0.95	3.1	0.77–6.9	3.6	1.0–8.3

S3.2 Respiratory CO_2 production rate vs CO_2 flux

CO_2 production rates were estimated from incubations for O_2 community respiration and compared to measured CO_2 fluxes for river (Fig. S5), channel (Fig. S6) and lake stations (Fig. S7). CO_2 fluxes (F_{CO2}) marked with a triangle were calculated using the median k_{600} from the measurements in the respective waterscape. Dark purple bars represent measured respiration rates (R), light purple bars indicate the effect of a correction with a factor of 2.7 for measurement limitations using BOD bottles (R_{corBOD}) according to Ward et al. (2018). Station numbers refer to the sampling locations displayed in Figure 1 in the main text and documented further in Table S1.

While respiration rate exceeds CO_2 flux in most cases in the River stations, the opposite is the case at many occasions in the channels, especially in the first half of the year until July. Respiration rates lower than CO_2 flux indicate an additional CO_2 source CO_2 source. The channels are in close contact with adjacent reed beds, and lateral inflow from these wetlands could explain the CO_2 excess.

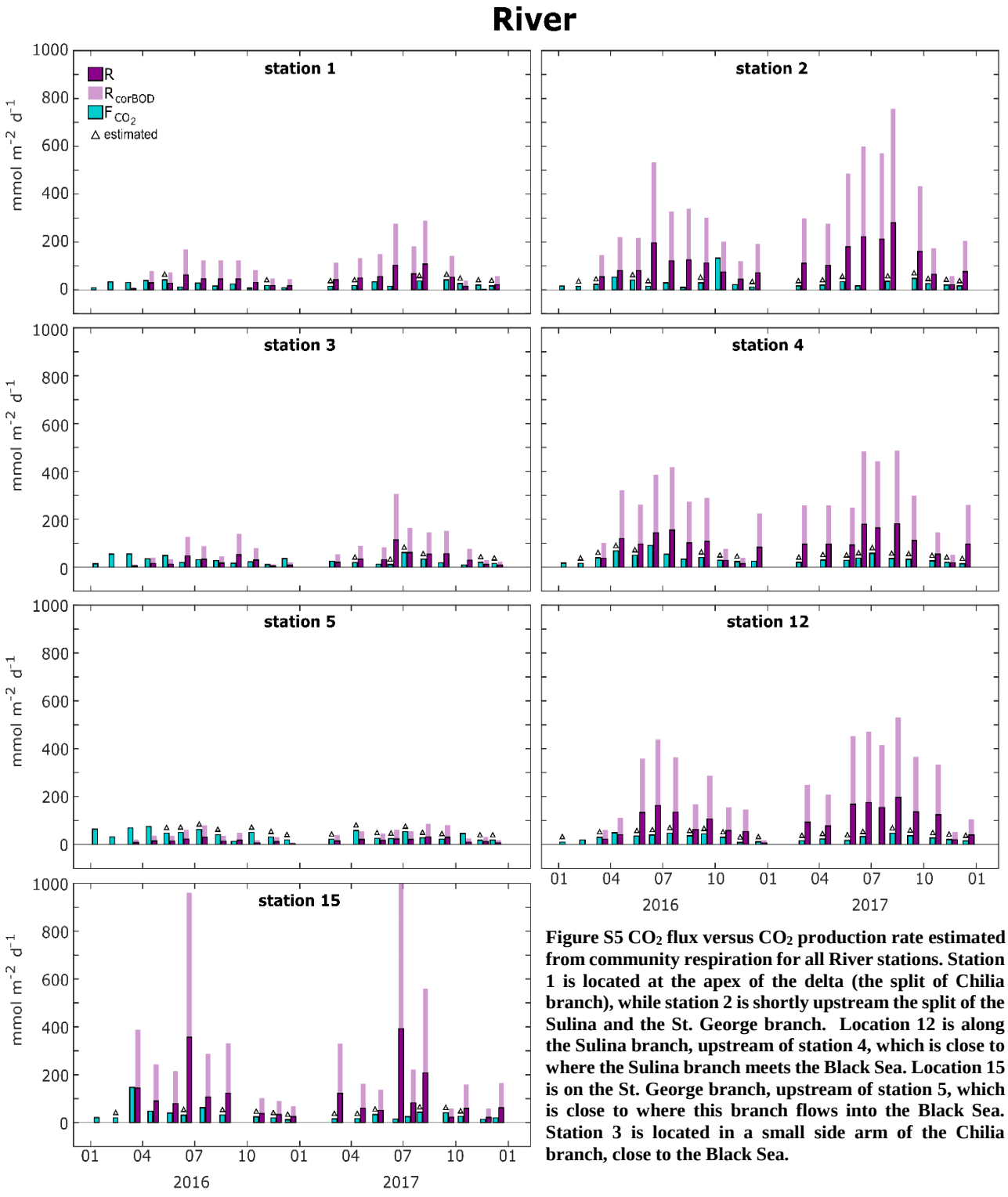

Figure S5 CO_2 flux versus CO_2 production rate estimated from community respiration for all River stations. Station 1 is located at the apex of the delta (the split of Chilia branch), while station 2 is shortly upstream the split of the Sulina and the St. George branch. Location 12 is along the Sulina branch, upstream of station 4, which is close to where the Sulina branch meets the Black Sea. Location 15 is on the St. George branch, upstream of station 5, which is close to where this branch flows into the Black Sea. Station 3 is located in a small side arm of the Chilia branch, close to the Black Sea.

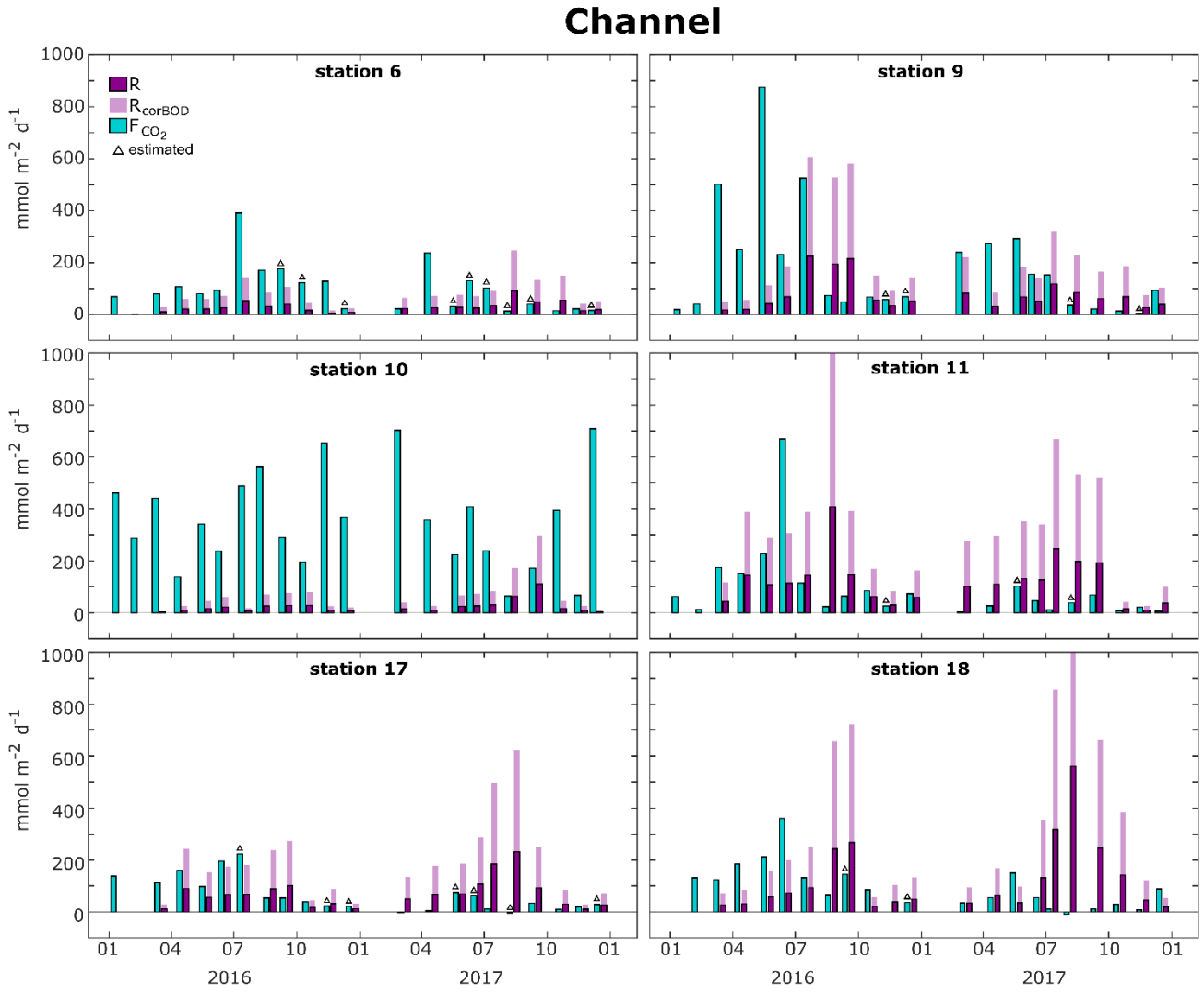

Figure S6 CO_2 flux versus CO_2 production rate estimated from community respiration for all channel stations. Station 6 and 9 are channels draining the delta towards the St.George and the Sulina branch, respectively. Station 10 is located at the border of a UNESCO biosphere reserve core protection zone and represented the CO_2 hotspot of this study. Station 11 and station 17 are old meanders of the Sulina branch. Station 18 is leading water from the Sulina branch into the delta. Both station 9 and station 18 are located in channels that are known to reverse flow direction.

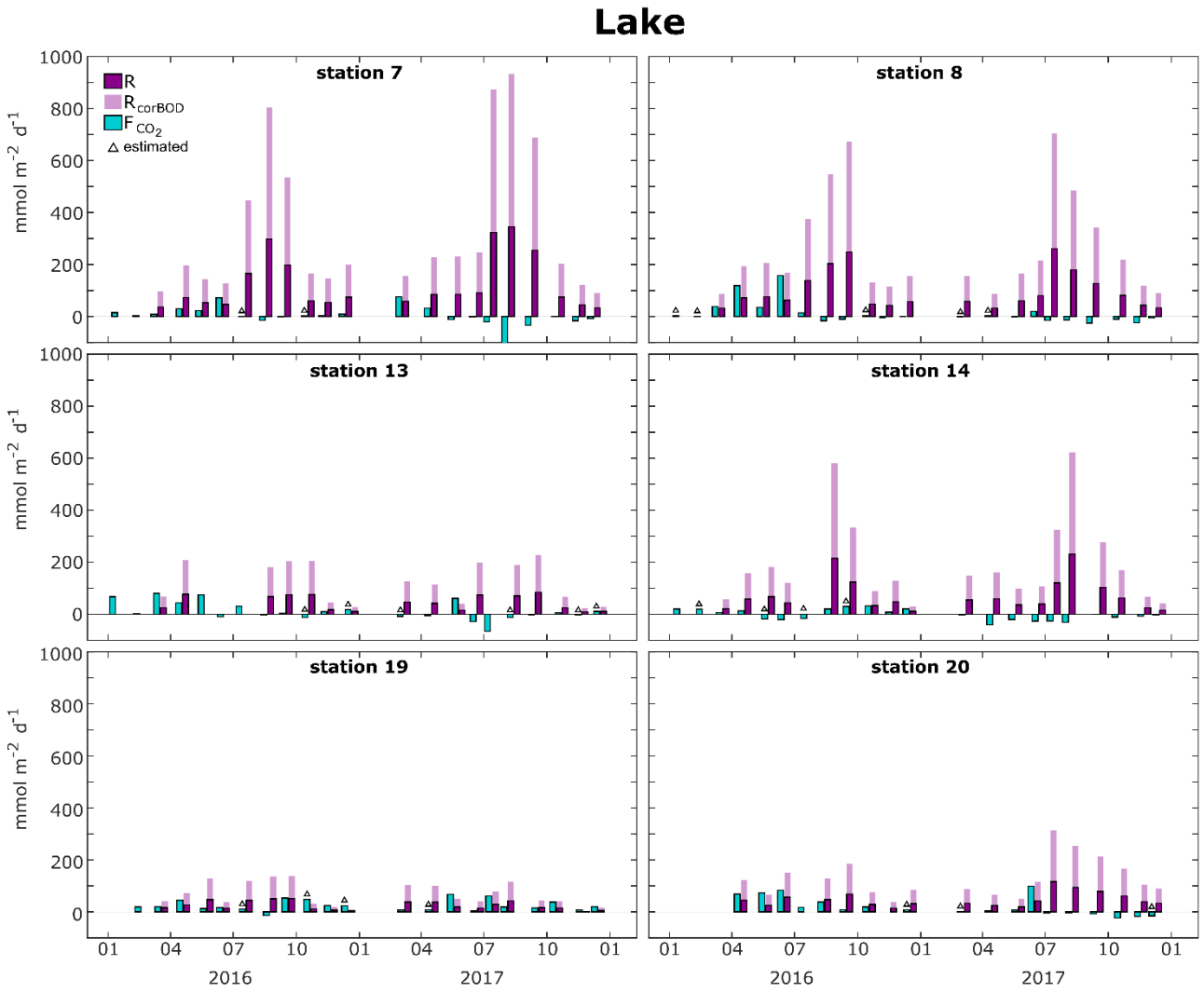

Figure S7 CO_2 flux versus CO_2 production rate estimated from community respiration for all lake stations. Station 14 and 19 are located in the Lake Uzlina-Isac complex, Station 7, 8 and 20 are located in the Lake Puiu-Rosu complex. Lake 13 is the only investigated lake north of the Sulina branch and located in the Matita-Merhei complex. Lake complexes as presented in Oosterberg et al. (2000).

S3.3 Estimating uncertainties related to hot spots and isolated lakes and their effect on atmospheric carbon fluxes

S3.3.1 Estimating the effect of potential hot spot channels

One of the channel stations (location 10, Fig. 1 main paper) showed very high CO_2 and elevated CH_4 concentrations during our observations. This location is draining a region with reed stands that are classified as strictly protected area by the Danube Delta Biosphere Reserve Authority (Fig. S8). The observation station itself is located in the buffer area surrounding the strictly protected area. Considering these two characteristics, i) more or less west-east drainage and ii) connection to either strictly protected area or buffer area, we estimate the fraction of potential hotspot channels to up to 2 % (Fig. S8). This approach assumes the hotspot conditions prevail along the whole channel and not just in the sampled cross-section.

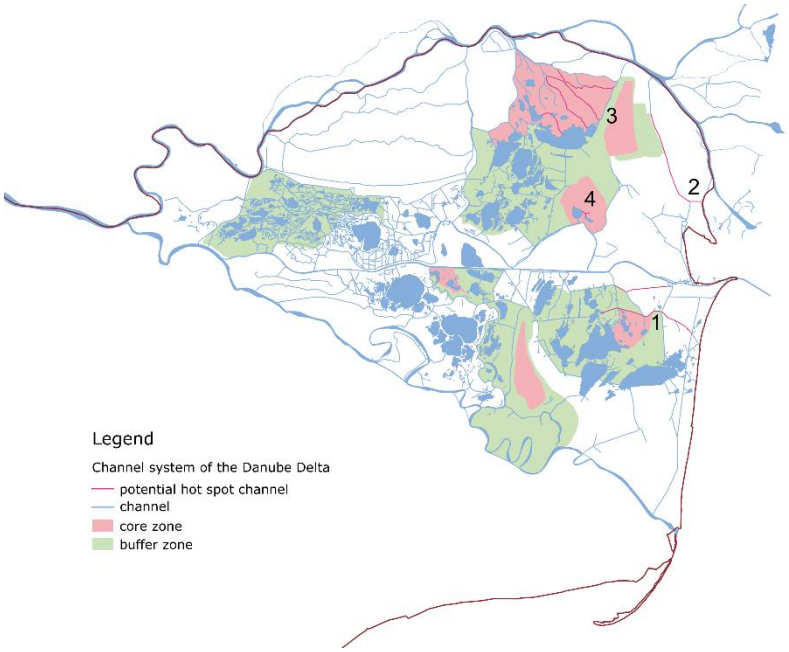

Figure S8 Channel system of the Danube Delta. Potential hotspot channels are indicated in purple. 1) The channel at location 10, where we observed high CO_2 concentrations. 2) EXO2 sensor data (not shown in this paper) indicated that this channel also has very high CO_2 concentrations. 3) and 4) channels within strictly protected area draining more or less west-east direction. Red and green shaded areas indicate core protection zones (red) and buffer areas (green) of the Danube Delta Biosphere Reserve between the three main branches of the Danube River. Protection zones redrawn from a map of the Danube Delta Biosphere Reserve Authority (2018), shape files for map creation in QGIS adapted from mapcruzin.com (Contains information from www.openstreetmap.org, which is made available here under the Open Database License (ODbL), https://opendatacommons.org/licenses/odbl/1.0/).

Assuming that 2 % of the channels' surface area are hotspots, the upscaling exercise suggests that the hotspots could contribute up to ~20 % to the CO_2 and total CH_4 fluxes from the channels (Fig. S9 and Table S3). However, the median flux for the channels decreased slightly in this example (cf. Table 2, main text), since the hotspot measurements are no longer pooled with the rest of the channel data and thereby the individual median fluxes used for the calculations of the rest of the channel surface area are slightly lower.

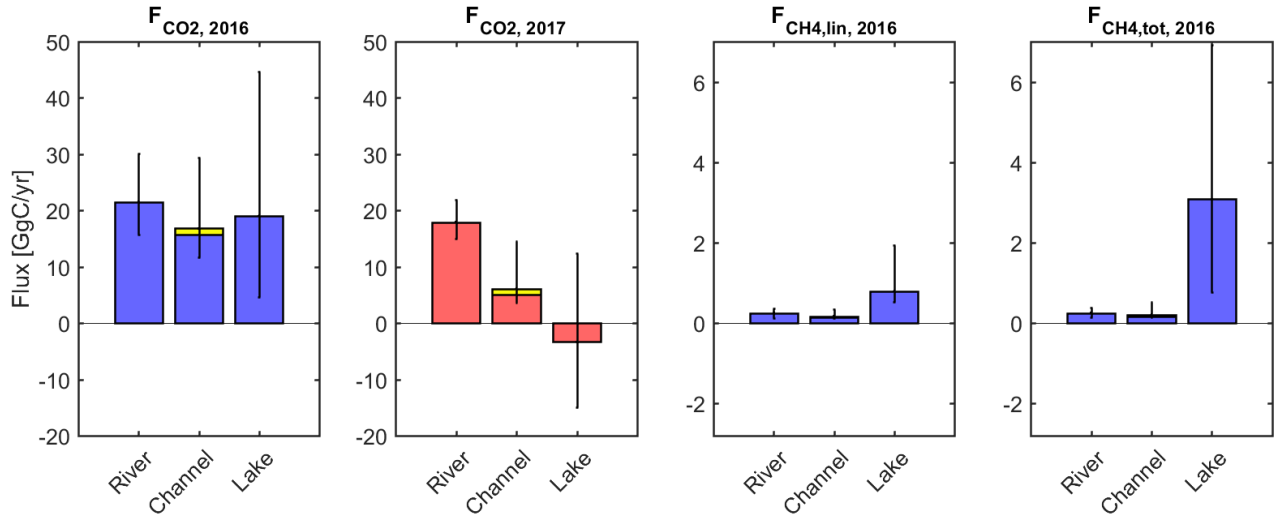

Figure S9 CO_2 and CH_4 flux (GgC yr^{-1}) from the delta's freshwaters in 2016 and 2017 considering 2 % of the channel area as hotspot. The indices lin and tot for CH_4 data indicate the diffusive emissions calculated from the linear increase and the total emissions including ebullition. For the channels, contributions from the hotspots are indicated in yellow. In case of CH_4, the yellow part of the bar is not visible, yet the hotspots still contribute 14 % and 18 % to the diffusieve and total flux, respectively (see Table S3).

Table S3 Total CO_2 and CH_4 flux (GgC yr^{-1}) from the delta's freshwaters in 2016 and 2017 considering 2% of the channel area as hotspot. For CH_4 both diffusive and total fluxes are displayed. Because of large data gaps in CH_4 no fluxes were calculated for 2017.

Flux	River		Channel			Lake	
[GgC yr^{-1}]	median	range	median	range	Frac hot spot [%]	median	range
$CO_{2,\ 2016}$	22	16–30	17	12–29	6.5	19	4.6–45
$CO_{2,\ 2017}$	18	15–22	6.1	3.7–15	18	-3.3	-15–12
$CH_{4,\ dif,\ 2016}$	0.25	0.13–0.36	0.17	0.12–0.34	14	0.79	0.52–1.9
$CH_{4,\ tot,\ 2016}$	0.25	0.15–0.39	0.21	0.15–0.53	18	3.1	0.77–6.9

S3.3.2 Estimating the effect of potentially isolated lakes

There are several reports in the literature that refer to some of the delta lakes as "isolated", receiving water from the reed bed and having a long residence time compared to the highly connected lakes. We used the references in Tudorancea and Tudorancea (2006), Covaliov and Coops (2003), the assessment of lake regimes in Oosterberg et al. (2000) and a land use map indicating isolated lakes presented in a report by Doroftei et al. (2013) for our estimation of the surface area of these isolated lakes.

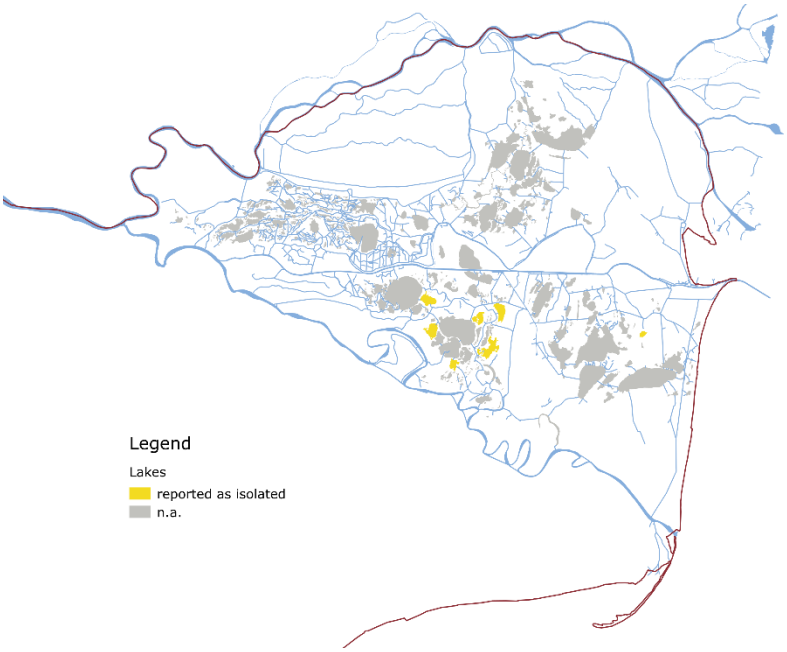

Figure S10 Isolated lakes of the Danube Delta mentioned in Tudorancea and Tudorancea (2006) and Covaliov and Coops (2003). Shape files for map creation in QGIS adapted from mapcruzin.com (Contains information from www.openstreetmap.org, which is made available here under the Open Database License (ODbL), https://opendatacommons.org/licenses/odbl/1.0/).

5

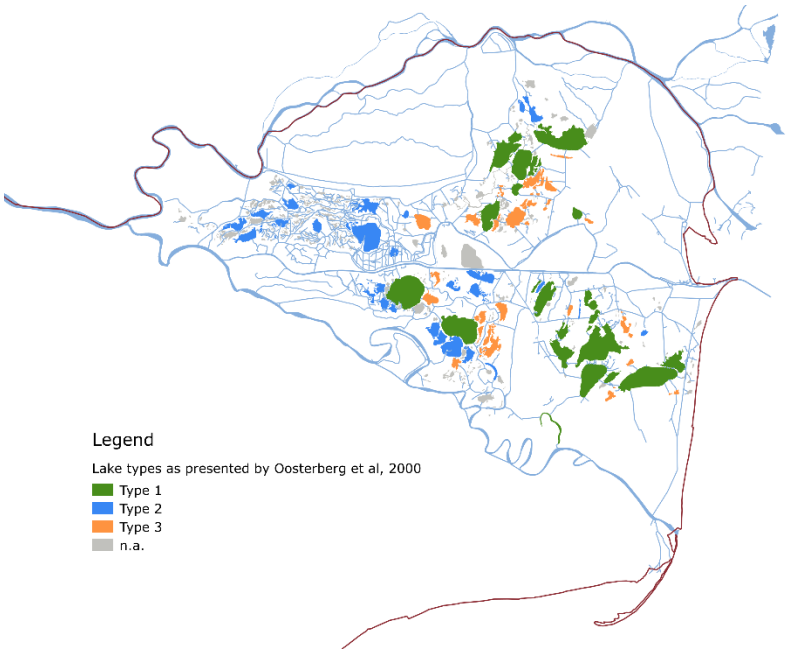

Figure S11 Typology of the delta lakes as presented by Oosterberg et al. (2000). Type 3 refers to isolated lakes with a high organic loading. Shape files for map creation in QGIS adapted from mapcruzin.com (Contains information from www.openstreetmap.org, which is made available here under the Open Database License (ODbL), https://opendatacommons.org/licenses/odbl/1.0/).

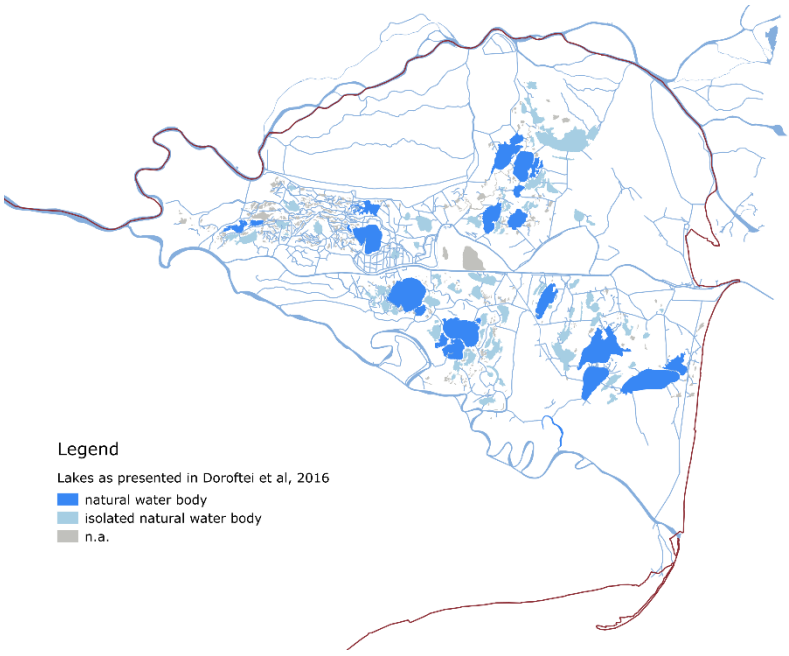

Figure S12 Isolated and non-isolated natural water bodies as presented by Doroftei et al. (2013) based on data from the Danube Delta Biosphere Reserve Authoriy. Shape files for map creation in QGIS adapted from mapcruzin.com (Contains information from www.openstreetmap.org, which is made available here under the Open Database License (ODbL), https://opendatacommons.org/licenses/odbl/1.0/).

The total surface area of the lakes presented as isolated in the above-mentioned studies (see Fig. S10, S11 & S12) amounts to 99 km^2. Studies on very small lakes with surface areas < 0.2 km^2 were not present in the literature. While small lakes represent the dominant type of lakes in the delta (75% of the lakes), their surface area amounts to only 7% (17.8 km^2). These lakes are likely also isolated, yet we do not consider them in the following scenario analysis. Attributing hotspot like flux characteristics to the isolated lakes (A = 99 km^2), indicates that they could strongly increase both CO_2 and CH_4 fluxes from the lakes and also reverse the potential sink capacity of the lakes in 2017 (Fig. 5 main text and Fig. S13). It is however unlikely that all isolated lakes have fluxes as high as the hotspot, so the evaluation of this scenario represents an upper boundary to the potential fluxes from these poorly characterized, isolated systems.

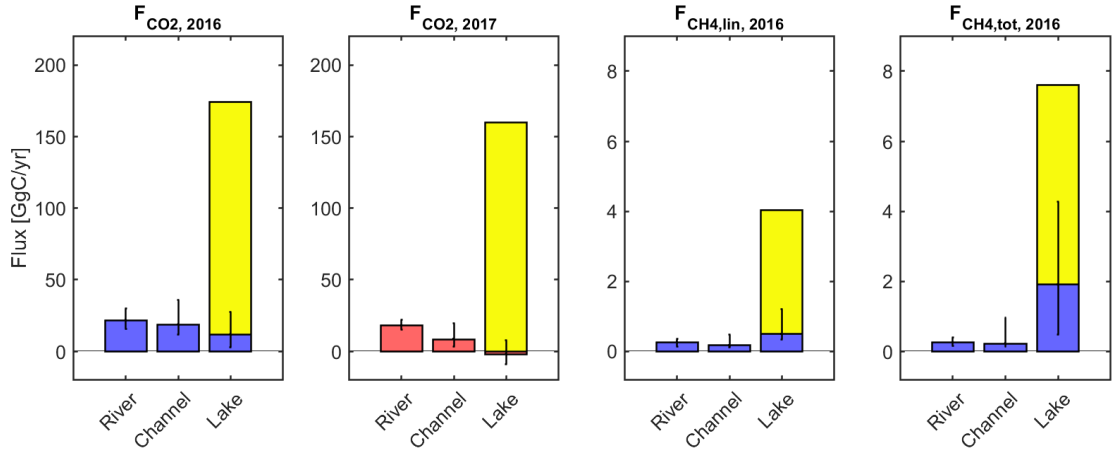

Figure S13 Total CO_2 and CH_4 flux (GgC yr^{-1}) from the delta's freshwaters in 2016 and 2017 considering isolated lakes covering 99km^2 as characterized by hotspot like fluxes. Estimated upper boundary for the contributions from the isolated lakes are shown in yellow.

Table S4 Total CO_2 and CH_4 flux (GgC yr^{-1}) from the delta's freshwaters in 2016 and 2017 considering 99km^2 as isolated lakes with hotspot like fluxes. For CH_4 both diffusive and total fluxes are displayed. Because of large data gaps in CH_4 no fluxes were calculated for 2017.

Flux	River		Channel		Lake		
[GgC yr^{-1}]	median	range	median	range	median	range	Frac isoLakes [%]
$CO_{2,\ 2016}$	22	16–30	19	12–36	174	165–190	93
$CO_{2,\ 2017}$	18	15–22	8.4	3.0–19	158	150–167	101[a]
$CH_{4,\ dif,\ 2016}$	0.25	0.13–0.36	0.16	0.11–0.48	4.0	3.9–4.7	88
$CH_{4,\ tot,\ 2016}$	0.25	0.15–0.39	0.22	0.13–0.95	7.6	6.2–10	75

[a] isolated lakes counteract the sink capacity of the flow-through lakes in this case.

References

Covaliov, S., & Coops, H. (2003). *Seasonality of aquatic vegetation in the Danube Delta*. Retrieved from Institute for Inland Water Management and Waste Water Treatment RIZA:

Danube Delta Biosphere Reserve Authority. (2018). DDBRA Map. Retrieved from http://www.ddbra.ro/en/ddbra-map

Doroftei, M., Mierla, M., Silviu, C., Nanu, C., & Lupu, G. (2013). *HABIT-CHANGE: Climate change adapted management plan for Danube Delta Biosphere Resereve*. Retrieved from http://www.habit-change.eu/fileadmin/results/HABIT-CHANGE_5_3_1g_DDNI_CAMP_for_Danube_Delta_BR.pdf

ICPDR. (2018). Danube River Basin Water Quality Database. Retrieved 02.02.2018 http://www.icpdr.org/wq-db/

mapcruzin.com. (2016). Retrieved 13.01.2016 https://mapcruzin.com/free-romania-arcgis-maps-shapefiles.htm, based on www.openstreetmap.org/

Oosterberg, W., Staras, M., Bogdan, L., Buijse, A. D., Constantinescu, A., Coops, H., . . . Navodaru, I. (2000). Ecological gradients in the Danube Delta lakes: present state and man-induced changes.

Tudorancea, C., & Tudorancea, M. M. (2006). *Danube Delta: genesis and biodiversity*. Leiden: Backhuys Publishers.

Ward, N. D., Sawakuchi, H. O., Neu, V., Less, D. F. S., Valerio, A. M., Cunha, A. C., . . . Keil, R. G. (2018). Velocity-amplified microbial respiration rates in the lower Amazon River. *Limnology and Oceanography Letters, 3*(3), 265-274. doi:doi:10.1002/lol2.10062